Current Research in Toxicology 7 (2024) 100195

Contents lists available at ScienceDirect

Current Research in Toxicology

journal homepage: www.journals.elsevier.com/current-research-in-toxicology

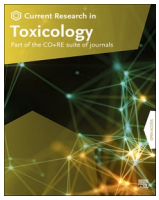

Research Paper

Subcellular expression of CYP2E1 in HepG2 cells impacts response to free oleic and palmitic acid

Zaria K. Killingsworth [a], Kelly R. Misare [a], Abigail S. Ryan [a], Elizabeth A. Ampolini [a], Tsultrim T. Mendenhall [a], Melinda A. Engevik [b,c], Jessica H. Hartman [a,b,*]

[a] Department of Biochemistry and Molecular Biology, Medical University of South Carolina, Charleston, SC, United States
[b] Department of Regenerative Medicine and Cell Biology, Medical University of South Carolina, Charleston, SC, United States
[c] Department of Microbiology and Immunology, Medical University of South Carolina, Charleston, SC, United States

ARTICLE INFO

Keywords:
CYP2E1
Free fatty acids
Palmitic acid
Oleic acid
Mitochondria

ABSTRACT

Aims: Cytochrome P450 2E1 (CYP2E1) is a mammalian monooxygenase expressed at high levels in the liver that metabolizes low molecular weight pollutants and drugs, as well as endogenous fatty acids and ketones. Although CYP2E1 has been mainly studied in the endoplasmic reticulum (ER, microsomal fraction), it also localizes in significant amounts to the mitochondria, where it has been far less studied. We investigated the effects of CYP2E1 expression in mitochondria, endoplasmic reticulum, or both organelles in transgenic HepG2 cells exposed to free oleic and palmitic acid, including effects on cytotoxicity, lipid storage, respiration, and gene expression.

Results: We found that HepG2 cells expressing CYP2E1 in both the ER and mitochondria have exacerbated levels of palmitic acid cytotoxicity and inhibited respiration. CYP2E1 expression did not impact lipid accumulation from fatty acid exposures, but mitochondrial CYP2E1 expression promoted lipid droplet depletion during serum starvation. In contrast to HepG2 cells, differentiated HepaRG cells express abundant CYP2E1, but they are not sensitive to palmitic acid cytotoxicity. Oleic acid exposure prompted less cytotoxicity, and CYP2E1 expression in the ER prevented an oleic-acid-induced increase in respiration. HepG2 cells exposed to mixtures of palmitic and oleic acid are protected from palmitic acid cytotoxicity. Additionally, we identified that CYP2E1 was decreased at the gene and protein level in hepatocellular carcinoma. Moreover, patients with tumors that had higher CYP2E1 expression had a better prognosis compared to patients with lower CYP2E1 expression.

Innovation: This study has demonstrated that transgenic CYP2E1 subcellular localization plays an important role in sensitivity to cytotoxicity, lipid storage, and respiration in the hepatoma cell line HepG2 exposed to palmitic and oleic acid. HepaRG cells, in contrast, were insensitive to palmitic acid. This work demonstrates the clear importance of CYP2E1 in dictating lipotoxicity and differential roles for the mitochondrial and ER forms of the enzyme. Additionally, our data supports a potentially unique role for CYP2E1 in cancer cells.

Conclusion: There lies a role for CYP2E1 in altering lipotoxicity, and since CYP2E1 is known to be upregulated in both liver disease and hepatocellular carcinoma, it is important to better define how the role of CYP2E1 changes during disease progression.

Introduction

Cytochrome P450 2E1 (CYP2E1) is a monooxygenase enzyme that is expressed at high levels in liver hepatocytes and is also expressed in many other tissues including kidneys, lung, heart, and brain (Miller, 2008; Roberts et al., 1994; Yadav et al., 2006). CYP2E1 is unique to mammals, is highly conserved among mammalian species, and has no known loss-of-function polymorphisms in the human population (Miller, 2008). CYP2E1 is tightly linked to metabolism, as it is induced in diabetes (Wang et al., 2003), obesity (Raucy et al., 1991; van Rongen et al., 2016; Khemawoot et al., 2007), fasting (Wan et al., 2006; Hong et al., 1987; Wang et al., 2022), and non-alcoholic fatty liver disease (Weltman et al., 1998; Harjumäki et al., 2021), presumably by high levels of circulating fatty acid and ketones (Bondoc et al., 1999). However, the extent and importance of CYP2E1 metabolism in these conditions is not well understood.

* Corresponding author.
E-mail address: hartmanj@musc.edu (J.H. Hartman).

https://doi.org/10.1016/j.crtox.2024.100195
Received 10 May 2024; Received in revised form 29 August 2024; Accepted 20 September 2024
Available online 28 September 2024

CYP2E1 has primarily been studied in the endoplasmic reticulum, but it localizes in significant amounts to the mitochondria (Hartman et al., 2017; Neve and Ingelman-Sundberg, 1999; Robin et al., 2001), where it has been far less studied. In each organelle, CYP2E1 has unique co-enzymes required for activity: in the endoplasmic reticulum, CYP2E1 associates with cytochrome P450 reductase (CPR), while in the mitochondria, CYP2E1 pairs with adrenodoxin and adrenodoxin reductase. We previously showed that CYP2E1 has unique enzyme kinetics in each organelle (Hartman et al., 2015). In the endoplasmic reticulum, CYP2E1 displays non-Michaelis-Menten kinetics for metabolism of many substrates, while in the mitochondria the activity as a function of substrate concentration is hyperbolic (Michaelis-Menten kinetics). Previous studies reported that transgenic expression of mitochondrial CYP2E1 exacerbated ethanol toxicity *in vitro* in Cos-7 kidney cells (Bansal et al., 2013; Bansal et al., 2010). We have also previously reported that high mitochondrial (but not ER) CYP2E1 expression was correlated with more impairment of the mitochondrial electron transport chain after *in vivo* exposure to 1,3-butadiene (Hartman et al., 2017). Together, these findings suggest that CYP2E1 activity can have unique kinetics and consequences for different cells/tissues/organisms.

CYP2E1 metabolizes many low-molecular weight pollutants (e.g. benzene (Bernauer et al., 1999), 1,3-butadiene (Nieusma et al., 1998), styrene (Hartman et al., 2012), dimethylnitrosamine (Dicker and Cederbaum, 1991) and drugs (ethanol (Lieber and DeCarli, 1970), acetaminophen (Akakpo et al., 2022), isoniazid (Huang et al., 2003), as well as endogenous compounds such as ketones and fatty acids (Miller, 2008). CYP2E1 has been demonstrated to primarily hydroxylate fatty acids at the omega-1 (preferred) and omega positions, which can lead to formation of dicarboxylic acids (Adas et al., 1998; Clarke et al., 1994). Prior research has connected CYP2E1 expression to toxicity of free fatty acids including palmitic acid, potentially through ER stress mechanisms. However, it is unknown what role subcellular-targeted CYP2E1 plays in mediating cellular response to free fatty acids.

In this study, we generated HepG2 cell lines expressing mitochondrial- and ER-targeted CYP2E1 by introducing previously validated point mutations (Bansal et al., 2013) into the N-terminal targeting sequence of CYP2E1 and transducing cells with lentivirus. We then used monoclonal lines expressing mtCYP2E1 and erCYP2E1 and compared these lines to HepG2 cells and an existing HepG2-CYP2E1 cell line transduced with the native sequence that localizes to both mitochondria and endoplasmic reticulum. We exposed cells to palmitic acid, oleic acid, or a mixture of both fatty acids and measured cytotoxicity, respiration, fat droplet accumulation, and gene expression for several genes related to lipids, antioxidant response, and ER stress. Overall, this study gives important new insights into the consequences of CYP2E1 activity in different cellular compartments on cellular response to free fatty acids.

Materials and Methods

Chemicals. Palmitate sodium salt (Cat# P9767), Oleate sodium salt (Cat# O7501), Nile Red (Cat# 19123) and Puromycin (Cat# P9620) were purchased from Sigma-Aldrich (St. Louis, MO). Fatty acid-free Bovine Serum Albumin (Cat# AAJ6494418) and 16 % Paraformaldehyde Solution (AA433689L) were purchased from Fisher Scientific (Waltham, MA).

Cell lines

The HepG2 cell line was obtained from MUSC Cell Models Core (MUSC DDRC Analytical Cell Model Core). The HepG2 cell line expressing CYP2E1 was a kind gift from Dr. Mitchell McGill (University of Arkansas for Medical Sciences, Little Rock, AR). The cell lines expressing CYP2E1 in the endoplasmic reticulum (ER-CYP2E1) and mitochondria (MT-CYP2E1) were created with the use of lentiviral constructs to express CYP2E1 in the specific organelles of interest. The lentivector plasmid (pLenti-GIII-CMV-CYP2E1) was obtained from Applied Biological Materials (ABM, Richmond, BC, Canada). Site-directed mutagenesis was used to introduce mutations to the N-terminal targeting sequence of the protein to cause amino acid changes to target CYP2E1 to mitochondria (V8R/V11R/L17R) or endoplasmic reticulum (A3L/A11L) (Bansal et al., 2012). The mutated lentivectors were verified by sequencing analysis and then packaged into live viral particles by the Duke Viral Core (Duke University, Durham, NC). HepG2 cells were infected at a MOI of 10 (the lowest MOI with surviving cells) and selected with puromycin (1 μg/mL). Monoclonal cell lines were obtained by cell dilution to single cells and re-expansion. Expression of CYP2E1 was verified by qPCR and immunofluorescent staining. Cells from each line were fixed and stained with Hoechst (BD Pharmigen, 561908) and rabbit anti-CYP2E1 (Abcam, ab28146), sheep anti-calreticulin (endoplasmic reticulum marker, ThermoFisher, Z100P), and chicken anti-HSP60 (mitochondrial marker, Bio-Techne, NBP3-05536). Alexa Fluor secondary antibodies were used to visualize the proteins, including donkey anti-rabbit Alexa Fluor 555, donkey anti-sheep Alexa Fluor 647, and donkey anti-chicken Alexa Fluor 488, respectively. Coverslips were mounted on slides with ProLong Glass Antifade Mountant (RI = 1.52, Invitrogen). For quantification of CYP2E1 signal, 10 images were acquired of each cell line at 200X magnification using a Leica DMi8 Thunder Imaging system and were cleared with Thunder deconvolution. We also used the software to quantify the CYP2E1 fluorescent intensity across each image. Nuclei counts for each image were quantified with ImageJ cell counter tool, and fluorescent intensity was normalized to cell count.

Undifferentiated, proliferating HepaRG cells were obtained from BioPredic International (Saint Gregoire, Bretagne, France) (Marion et al., 2010). Cells were maintained/passaged and subsequently differentiated for experiments. Differentiated and undifferentiated cells were tested for CYP2E1 expression using immunofluorescent staining and ProteinSimple automated western blotting (Lück et al., 2021) with rabbit anti-CYP2E1 (Abcam, ab28146) according to manufacturer's instructions (ProteinSimple, San Jose, CA). Data was analyzed using Compass for Simple Western software. Immunofluorescence was visualized using Airyscan super-resolution confocal fluorescent imaging was performed using a Zeiss LSM 880 Axio Examiner confocal microscope (Zeiss, Germany) at 630X magnification (objective Plan-Apochromat 63x/1.4 Oil DIC M27). Z stacks were taken with optimal Nyquist sampling. Images were deconvolved using the Airyscan deconvolution and maximum projections were prepared for visualization.

Cell culture

HepG2-derived cells were cultured in RPMI 1640 with L-glutamine (Gibco, Thermo Fisher Scientific, Waltham, MA). Growth media for HepG2 and CYP2E1 cell lines contained added penicillin/streptomycin antibiotics (Gibco, Thermo Fisher Scientific, Waltham, MA) and 10 % fetal bovine serum (FBS, VWR Seradigm, Radnor, PA). Selection media for MT and ER lines contained added 10 % FBS, 1x penicillin/streptomycin, and 1 μg/mL puromycin (puromycin dose determined empirically for optimal selection of lentiviral-transduced cells). Cells were maintained at 37°C with 5 % CO_2 atmosphere in a humidified incubator.

HepaRG cells were cultured in Williams E media supplemented with GlutaMAX (Gibco, ThermoFisher Scientific) and the HepaRG Maintenance/Metabolism Supplement (BioPredic International, Saint Gregoire, Bretagne, France) and passaged when they reached near confluency. They were then seeded into 96-well plates and allowed to reach confluency for two weeks in Maintenance Medium, then switched to Williams E media supplemented with GlutaMAX (Gibco, ThermoFisher Scientific) and the HepaRG Differentiation Supplement for two additional weeks. Differentiated cells were exposed to FFA after the four weeks of differentiation.

Fatty acid exposures

For fatty acid exposures, cells were dosed with 0.1 mM, 0.25 mM, and 0.5 mM FFA in 0.5 % ethanol and 1 % fatty acid-free bovine serum albumin (BSA) for 24 h or 5-day durations. These concentrations have been used previously for *in vitro* studies of lipid accumulation in primary hepatocytes (Sharma et al., 2011; Wanninger et al., 2011), HepG2 cells (Cui et al., 2010; Gómez-Lechón et al., 2007), and HepaRG cells (Michaut et al., 2016). These concentrations are also in the range of fasting plasma concentrations of fatty acids in humans with and without Metabolic Dysfunction-Associated Steatotic Liver Disease (MASLD, formerly known as Nonalcoholic Fatty Liver Disease or NAFLD) (Belfort et al., 2006; Sanyal et al., 2001). Control wells contained 0.5 % ethanol and 1 % fatty acid-free BSA to control for any effects of BSA in the culture medium. In order to solubilize the fatty acids, 20X working solutions were prepared by heating 20 % BSA with the fatty acid at 50 °C for at least 15 min. During this time, the cloudy solution became translucent. The solution was then diluted in pre-warmed growth media and applied to cells. The 20 % BSA control solution was only heated to 37 °C to avoid precipitation of the BSA.

Cytotoxicity assays

The cells were once again treated for 24 h in the FLUOstar Omega plate reader (BMG LabTech) using propidium iodide fluorescence as a measure for cell lethality. Following the 24 h treatment, cells were lysed with 2 % Triton to quantify the total number of cells per well for standardization of data.

Nile Red staining for neutral lipids

Cells were seeded on 96-well micro clear flat bottom white-walled plates (Greiner Bio-One) and treated with PA, OA, or PA and OA mixtures for 24 h or 5-days. Cell media was not refreshed in either experimental condition. Following FFA exposures, cells were then stained for visualization. For lipid droplet (Santoro, Caprio et al.) and DNA labeling, cells were washed twice with phosphate buffered saline (Gibco, Thermo Fisher Scientific) and then fixed with 100 μL 4 % paraformaldehyde (PFA), incubating at room temperature for 10 min. Cells were washed twice again with PBS and stained with Nile Red (1 μM final) and DAPI (1 mg/mL final) in PBS, incubating at room temperature for 30 min. Following this, fluorescence was read four times over 15 min at 544 nm ex./620 nm em. (Nile Red) and 355 nm ex./460 nm em. (DAPI) at 37 °C. The fixed cells were imaged using the Leica DMI-8 Thunder Imager inverted microscope at 100X total magnification.

To quantify the lipid droplets found in the four cell lines dosed with palmitic acid, oleic acid, and physiological mixtures of the two, ImageJ FIJI analysis was conducted. The corresponding images from inverted microscopy were exported as raw images containing both the Nile Red and DAPI channels, including three images per well per 96-well plate. Three images per well were taken using a central focus and the three images, R1, R2, and R3 had their mean lipid droplets values averaged. For quantification of lipid droplets, Nile Red fluorescence was measured on the images using ImageJ FIJI analysis software. Nile Red fluorescence was normalized to total cell area to correct for cell number.

RNA extraction and qPCR

HepG2 cells and the CYP2E1-expressing cell lines were seeded at 300,000 cells/well and plated in 6-well plates to incubate for 1–2 days until cell confluency. After cell confluency was reached, the four cell lines were dosed with the desired free fatty acids and incubated for 24 h. Specifically, cells were dosed with a vehicle control (0.5 % ethanol and 1 % BSA), 0.25 mM PA, 0.5 mM OA, and 0.25 mM PA/0.5 mM OA. Non-lethal doses of palmitic acid were used to ensure that living cells were able to be examined for quantification of gene expression. The experiment was run in biological triplicate.

Following FFA exposure and 24 h incubation, cells were washed with sterile phosphate-buffered saline solution (Gibco, ThermoFisher Scientific). In order to extract RNA from the cells, the cells were scraped from the 6-well plates and spun down to produce pellets. The supernatant was aspirated before the cell pellets were flash frozen and stored at −80℃. Qiagen QiaShredder cell-lysate kit (Qiagen, Germantown, MD, USA, Cat. No. 79656) and Qiagen RNeasy Plus Mini kit (Qiagen, Germantown, MD, USA, Cat. No. 74134; with optional gDNA digestion with DNaseI) were used for the RNA isolation. Generated RNA was converted into cDNA using the AppliedBiosystems High-Capacity cDNA Reverse Transcription kit (Fisher scientific, Cat. No. 43–688-14) and concentrations were measured to determine the proper dilutions. Approximately 500 ng of extracted RNA was used in the synthesis of cDNA.

RT-qPCR was performed in 20 μL reactions containing 2 ng of cDNA and using Quantabio PerfeCTa SYBR Green FastMix Master Mix (Quantabio supplied by VWR, Cat. No. 101414–276). The AriaMx Real-Time PCR system (Agilent) was used for gene expression measurements. The gene expression calculations were performed by comparing the relative change in the cycle threshold value (ΔCt). Fold change in expression was calculated using the $2^{-\Delta\Delta Ct}$ method with β-actin as the primary housekeeping gene and normalized to the BSA controls for each cell line. A complete list of the genes of interest and their corresponding forward and reverse primers can be found in Table S1 in Supplemental Information. All primer sequences were obtained from the Origene qPCR human primer pairs list and blasted using the NCBI BLAST transcriptome to ensure proper specificity. All primers were obtained from Integrated DNA Technologies and shipped in ambient conditions (Integrated DNA Technologies, Morrisville, NC, USA).

Respiration (oxygen consumption rate) assays

Oxygen consumption rates were analyzed for HepG2 and the CYP2E1-expressing cell lines with the Lucid Scientific Resipher device (Lucid Scientific, Atlanta, GA, USA), maintained at 37 °C and 5 % CO_2. Oleic acid and BSA controls, as well as palmitic acid and BSA controls, were exposed to the four cell lines for 5-day increments while the 96-well plate remained connected with the Resipher lid containing sensing probes to measure OCR. Cells' baseline oxygen consumption rate before treatment was measured for 24 h (to allow cells to reach confluency) before free fatty acid exposures were introduced. Data analysis was conducted from four individual experiments and change in OCR was quantified across all time points.

Computational analysis

Several databases were used to analyze the levels of CYP2E1 mRNA in Liver Hepatocellular Carcinoma (LIHC). Data was collected using the input gene CYP2E1 in the Cancer Genome Atlas Program (TCGA) in the TNMplot database (https://tnmplot.com). CYP2E1 expression data from RNAseq was collected from both normal non-cancer samples, tumor adjacent normal samples, and tumor samples (Bartha and Győrffy, 2021). CYP2E1 mRNA in LIHC was examined using the UALCAN Database (https://ualcan.path.uab.edu) as previously described (Chen et al., 2019). The database contains demographics on patients' age, weight, ethnicity, tumor type, tumor stage, tumor grade, and tumor histology. Protein levels of CYP2E1 in LIHC were obtained from the Clinical Proteomics Consortium for Cancer Analysis (CPTAC) dataset via the UALCAN Database (https://ualcan.path.uab.edu) (Chen et al., 2019). The correlation between the gene expression of CYP2E1 and the Kaplan-Meier overall survival-based outcomes in human hepatocellular carcinoma were analyzed using the R2 Genomics Analysis and Visualization Platform (https://r2.amc.nl) (Tumor Liver Hepatocellular Carcinoma: TCGA n = 371). Chi, df and p values were provided by the database.

Statistical analysis

All analyses were performed using GraphPad Prism software, version 9. Differences were deemed significant at a P value of less than 0.05, or a confidence interval of 95 %. Graphical data displays the normalized mean (compared to control) and standard error of the mean. Statistical significance was determined using One- or Two-way ANOVA, as appropriate.

Results

Lentiviral transduction of HepG2 cells restores CYP2E1 expression

CYP2E1 is normally expressed at high levels in hepatocytes, particularly pericentral hepatocytes, but immortalized HepG2 cells have lost robust expression of this enzyme. After we transduced cells with lentivirus, we observed ~ 100-fold higher levels of mRNA (Fig. 1A) and ~ 2-fold increased immunofluorescence with an anti-CYP2E1 antibody (Fig. 1B-C). The CYP2E1 lines had some variation/mosaicism in expression among individual cells (see images in Fig. 1B), which is common in lentiviral transduction. Overall, the cell lines had similar levels of CYP2E1, allowing direct comparison of effects of free fatty acid exposures.

CYP2E1 expression in both organelles exacerbates palmitic acid cytotoxicity

When exposed to palmitic acid, all HepG2-derived cell lines had a dose-dependent increase in cytotoxicity (Fig. 2A). A two-way ANOVA (palmitic acid dose vs. cell line) revealed significant effects of cell line ($p = 0.0011$), dose ($p < 0.0001$), and interaction ($p = 0.0006$). Multiple comparison analysis of cytotoxicity at each dose compared to the HepG2 line revealed only significance in the CYP2E1 cell line expressing the enzyme in both organelles at the highest dose of 0.5 mM ($p < 0.0001$). Together, these results revealed CYP2E1 expression in both organelles to be a liability for palmitic acid toxicity. Based on these results, we decided to use 0.25 mM palmitic acid for analysis of lipid droplets and mitochondrial effects, as this dose caused minimal cytotoxicity in the lines.

Mitochondrial CYP2E1 expression promotes lipid droplet depletion during serum starvation

After assessing the cytotoxicity of palmitic acid, we wanted to test if palmitic acid would drive lipid droplet formation in the short term (24 h) and after serum starvation (5 days), when glucose stores would be depleted. We observed that at 24 h, all cell lines had a significant ~ 4-fold increase in lipid droplets as assessed by Nile Red fluorescence (Fig. 2B). After serum starvation, we observed a decrease in lipid droplets compared to 24 h in all cell lines, but most dramatically in the CYP2E1 and MT-CYP2E1 cell lines (Fig. 2C), which had significantly less Nile Red fluorescence compared to the HepG2 cell line at this time point. Conversely, the ER-CYP2E1 line had similar lipid droplets to the HepG2 line. Together, this suggests a role for MT-CYP2E1 in promoting lipid clearance from the cells.

Palmitic acid inhibits respiration only in cells expressing dual-targeted CYP2E1

We reasoned that since lipid droplets were depleted in the 5-day serum starvation more dramatically in cells expressing MT-CYP2E1, perhaps MT-CYP2E1 was somehow promoting beta-oxidation of those stored fatty acids. We therefore measured oxygen consumption rates over time for the 5 days of serum starvation using the passive continuous OCR monitoring Resipher device. Interestingly, we did not see a palmitic acid-induced increase in OCR in any cell line compared to the vehicle controls (Fig. 2D-G). Rather, we saw transient inhibition of respiration in the CYP2E1 cell line (Fig. 2E) and the ER-CYP2E1 (Fig. 2G), but we did not observe the same level of respiration in the HepG2 (Fig. 2D) nor MT-CYP2E1 (Fig. 2F) lines. These data suggest that lipid clearance does not alter the overall respiration rate in these lines. Based on these results, we next asked if the less cytotoxic and more lipogenic oleic acid would have a similar effect on our cell lines.

Oleic acid is less cytotoxic than palmitic acid to HepG2 cells

Compared to palmitic acid, oleic acid caused much less cytotoxicity, with the highest lethality observed in the CYP2E1 line with CYP2E1 targeted to both organelles (Fig. 3A). This significantly increased lethality was observed at both of the highest doses, 0.5 and 1 mM oleic acid. The other cell lines with CYP2E1 targeted to a single organelle did not experience increased sensitivity to oleic acid-induced cytotoxicity.

CYP2E1 expression does not impact lipid accumulation from oleic acid exposures

Similar to palmitic acid exposures, exposure of all HepG2-derived cell lines to oleic acid for 24 h resulted in accumulation of lipid droplets as determined by Nile Red staining (Fig. 3B). After 5 days, with serum starvation, there was a decrease in Nile Red staining (Fig. 3C) but not as dramatically as was observed for palmitic acid. At both 24 h and 5 days, the CYP2E1 cell line trended toward decreased lipid accumulation compared to HepG2 and MT-CYP2E1 cell lines (Fig. 3B-C, $p = 0.12$ and $p = 0.11$, respectively), although these differences did not reach statistical significance due to variability in the measurements. Overall, the accumulation of lipid within HepG2-derived cell lines with oleic acid exposures was not significantly impacted by CYP2E1 status.

Expression of CYP2E1 in the ER prevents oleic-acid-induced increase in respiration

As with palmitic acid, we wondered if free oleic acid exposures could fuel respiration, particularly during serum starvation. To test this, we used the Resipher device to continuously monitor oxygen consumption rates by the HepG2 cell lines with and without exposure to 0.5 mM oleic acid for 5 days (Fig. 3D-G). We observed that oleic acid stimulated respiration after ~ 3 days in both HepG2 (Fig. 3D) and MT-CYP2E1 (Fig. 3F) cell lines, but this increase was completely absent in ER-CYP2E1 (Fig. 3G) and the CYP2E1 (Fig. 3E) cell line that has both ER and mitochondrial CYP2E1. These intriguing data suggest that CYP2E1 localized in the ER prevented stimulation of respiration by oleic acid exposures. Based on these findings, we wanted to test what gene expression changes may be driving these differences.

Targeted gene expression analysis reveals few differentially expressed genes between cell lines with oleic acid exposures

Based on observed differences between cell lines, we measured mRNA expression of genes related to ER stress, lipid handling, and oxidative stress following a 24-hour exposure to palmitic acid and oleic acid. Surprisingly, the majority of the genes we tested were unchanged by treatment with palmitic acid (all genes, Supplemental Figure S1) or oleic acid (non-significant genes only, Supplemental Figure S2), or did not differ among cell lines. Of the six genes that were significantly different after oleic acid treatment, XBP1s (spliced and active form of XBP1, turned on during IRE1-dependent unfolded protein response) was 3-fold increased in the CYP2E1 line that also showed cytotoxicity from oleic acid (Fig. 4A, $p < 0.01$). By contrast, the other ER stress genes tested here (BiP, CHOP, MANF, and to a lesser extent ATF6) were downregulated by oleic acid in all cell lines (Supplemental Table 1). Fatty acid synthase (FAS) was downregulated during oleic acid exposures in CYP2E1-expressing cell lines, but unchanged in HepG2 cells

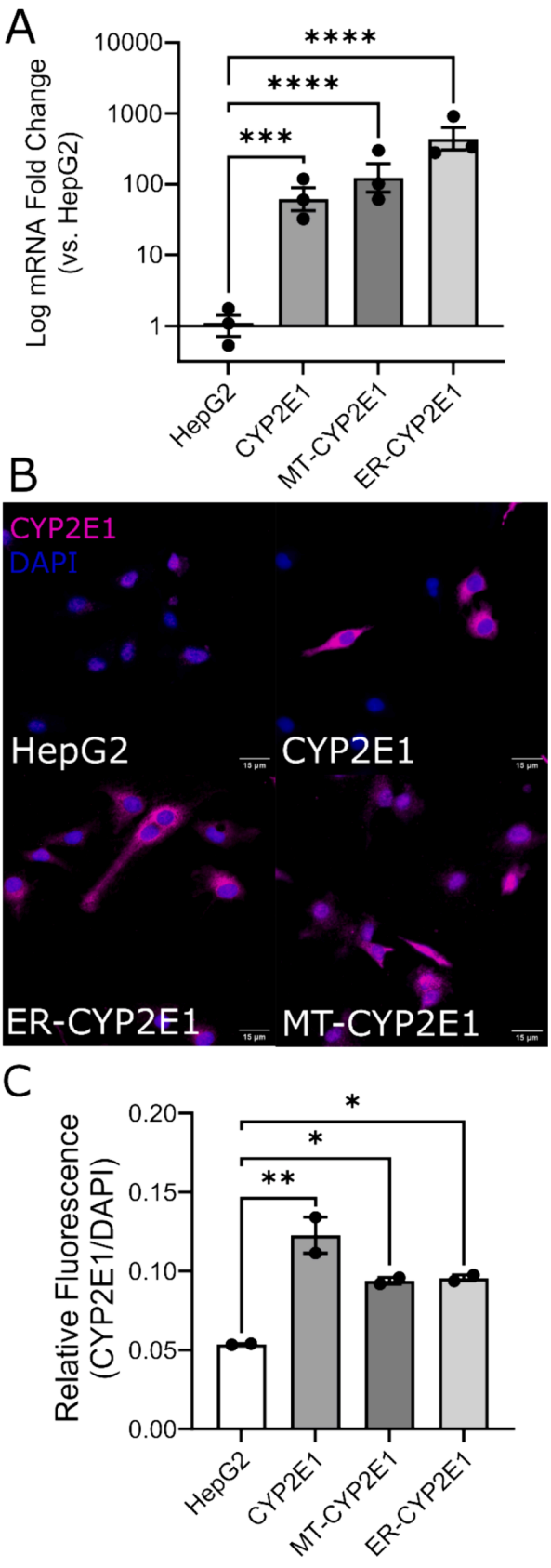

Fig. 1. Lentiviral transduction of HepG2 cells with CMV-CYP2E1 results in high expression of mRNA and modest induction of protein levels. To express CYP2E1 in HepG2 cells, lentiviral transduction was carried out at a MOI of 10, and transduced cells were selected with puromycin. Monoclonal lines were isolated and lines with similar mRNA and protein levels were selected for comparison. Panel A, mRNA expression of CYP2E1 determined by qPCR (normalized to B-actin). Data represent three independent experiments. Asterisks represent significance in one-way ANOVA post-testing with Dunnett's multiple comparison test compared to HepG2: ***, $p < 0.001$, ****, $p < 0.0001$. Panel B, immunofluorescent imaging of fixed cells stained for anti-CYP2E1 (Abcam 28146) and counterstained with DAPI. Panel C, relative fluorescence determined using ImageJ and normalized to the DAPI signal to control for number of cells. Data represent two independent experiments. Asterisks represent significance in one-way ANOVA post-testing with Dunnett's multiple comparison test compared to HepG2: * $p < 0.05$, **, $p < 0.01$.

(caption on next column)

(Fig. 4B, $p < 0.05$), while the gene encoding peroxisomal fatty acid degrading enzyme acyl-CoA oxidase (ACOX2) was increased in CYP2E1 and ER-CYP2E1 lines but decreased in HepG2 cells (Fig. 4C, $p < 0.01$). The cytosolic copper/zinc superoxide dismutase SOD1 was downregulated by oleic acid exposures in all treatment groups except for the CYP2E1 line (Fig. 4D, $p < 0.05$). By contrast, the mitochondrial manganese superoxide dismutase SOD2 was only downregulated in the CYP2E1 line and was unchanged in all other cell lines (Fig. 4E, $p < 0.05$). Together, the gene expression analysis is suggestive of differential responses to oleic acid, but further experiments including analyses at additional time points will be needed to tease apart these responses.

In mixtures of palmitic and oleic acids, oleic acid dominates the response

Because we saw such different results when we exposed cells to palmitic and oleic acids, we also tested their effects in mixtures, as oleic acid has been previously reported to be protective from palmitic acid cytotoxicity. We found that the mixture was not very cytotoxic, similar to oleic acid alone, and oleic acid co-exposure protected from the cytotoxicity observed at 0.5 mM PA (Fig. 5A), regardless of cell line. Also similar to oleic acid alone, all cell lines accumulated lipid droplets in response to the mixture of 0.25 mM PA and 0.5 mM OA after 24 h (Fig. 5B) and 5 days (Fig. 5C). Gene expression analysis revealed significant upregulation of the cytosolic copper/zinc superoxide dismutase SOD1 and thioredoxin (TXN) in the CYP2E1 line (Fig. 5D-E), similar to oleic acid. Also mirroring the oleic acid response, the fatty acid degrading enzyme acyl-CoA oxidase was significantly different between lines. The isoform ACOX1 was significant in the one-way ANOVA but not between groups (Fig. 5F), while the ACOX2 isoform was increased in CYP2E1 and ER-CYP2E1 lines but decreased in HepG2 cells (Fig. 5G). All other genes tested were not significantly different between cell lines (Supplemental Table S3). Together, these findings support that in a mixture of palmitic and oleic acid, the response and role of CYP2E1 seems to mirror that of its response to oleic acid alone.

Unlike HepG2 cells, HepaRG cells are not sensitive to palmitic acid cytotoxicity, regardless of CYP2E1 status

HepaRG cells are a co-culture of biliary cells and hepatocytes that are cancer-derived, but after 30 days of differentiation become more hepatocyte-like compared to HepG2 cells. As was previously reported, we found a dramatic increase in CYP2E1 levels in differentiated HepaRG cells compared to undifferentiated cells (Fig. 6A-D), with CYP2E1 protein levels increasing > 50-fold during differentiation. Surprisingly, we found that HepaRG cells were resistant to palmitic acid-induced cytotoxicity regardless of differentiation state, exhibiting < 10 % lethality even at doses that were highly cytotoxic to all HepG2 cells (Fig. 6E-F). Addition of the CYP2E1 irreversible inhibitor clomethiazole did not significantly change the lethality in differentiated or undifferentiated cells. Based on these findings, we conclude that CYP2E1-induced

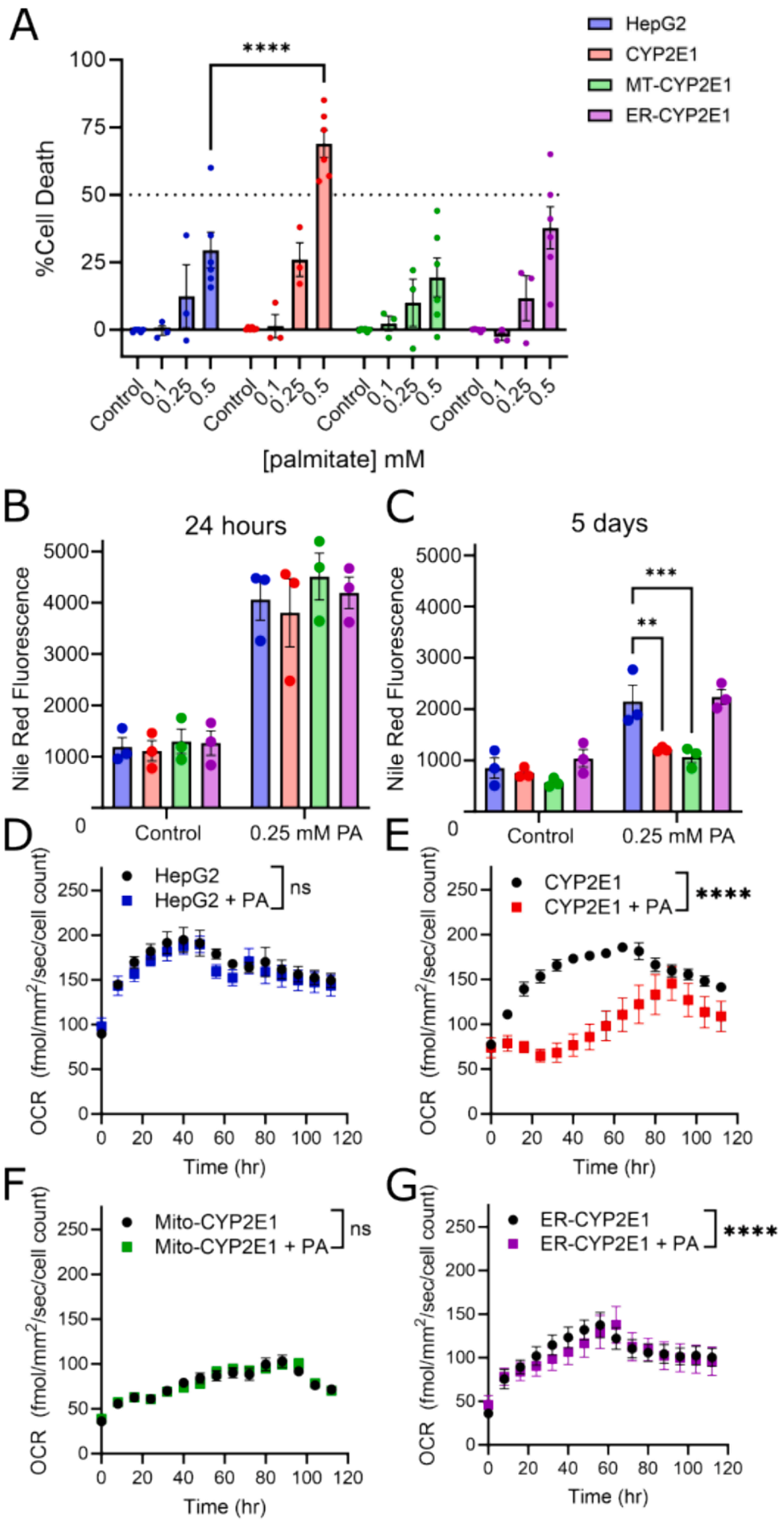

(caption on next page)

Fig. 2. CYP2E1 expression in HepG2 cells sensitizes to palmitic acid cytotoxicity and mitochondrial inhibition. Panel A, cell death following 24-hour exposure to palmitic acid was determined by propidium iodide fluorescence (normalized to total fluorescence after addition of 1 % Triton X-100). ****, $p < 0.0001$, adjusted for multiple comparisons after 2-way ANOVA. Panels B-C, lipid droplets were measured following a 24 h (fed, panel B) or 5-day (serum starved, panel C) exposure to 0.25 mM PA. Briefly, following the exposure cells were fixed with 4 % paraformaldehyde and stained with Nile Red. **, $p < 0.01$, ***, $p < 0.001$, adjusted for multiple comparisons after 2-way ANOVA. Panels D-G, real-time oxygen consumption rate during exposure to 0.25 mM PA was measured using a Resipher device from Lucid Scientific. ****, $p < 0.0001$ comparing area under the curve compiled from 3 independent replicates. (For interpretation of the references to colour in this figure legend, the reader is referred to the web version of this article.)

palmitate sensitivity is much more dramatic in the hepatocarcinoma cell line HepG2 compared to the more normal hepatocyte-like HepaRG cells.

Since our data suggest that our cells with a more cancer-like phenotype have less CYP2E1 and may be more sensitive to fatty acid stimulation in the presence of CYP2E1, we sought to identify the levels of CYP2E1 in normal liver and Liver Hepatocellular Carcinoma (LIHC). Analysis of mRNA in normal non-cancer samples revealed high expression of CYP2E1 in normal liver compared to LIHC tumors (Fig. 7A). We found a similar phenotype when we examined normal tumor adjacent liver, with normal liver exhibiting higher levels of CYP2E1 compared to LIHC tumors (Fig. 7B). We further analyzed the mRNA data based on tumor grade, stage, type, patient age, patient ethnicity, patient gender, and patient weight (Supplemental Fig. 2). We first examined tumor grade, which is based on the appearance of the cancer cells, with the higher grades appearing far different from the normal tissue. We found that CYP2E1 mRNA was decreased in grade 2, grade 3 and grade 4 LIHC tumors (Supplemental Fig. 2A), but relatively normal in grade 1 tumors. We next examined cancer stage, which is an indicator of where the cancer is in the body and how far it has spread. We found that CYP2E1 mRNA was decreased in all the stages of LIHC compared to the non-tumor controls (Supplemental Fig. 2B). Interestingly, CYP2E1 was decreased in hepatocellular and fibrolamellar carcinoma but remained at similar levels to the control in mixed heptaocholangio-carcinoma (Supplemental Fig. 2C). This suggests that CYP2E1 is tumor type dependent. In terms of patient status, we found that CYP2E1 mRNA was decreased in LIHC tumors regardless of age, ethnicity, gender and weight (Supplemental Figure D-G). Reflecting our mRNA findings, proteomic analysis demonstrated that CYP2E1 protein was decreased in LIHC tumors compared to non-tumor controls (Supplemental Fig. 2H). Finally, we found that patients with low CYP2E1 levels had worse overall survival compared to patients with high CYP2E1 expression (Fig. 7C). These data highlight the potential for CYP2E1 expression to be relevant to hepatic cancer progression and survival.

Discussion

In this study, we found that CYP2E1 expression in HepG2 cells sensitized them to palmitic acid cytotoxicity, an effect that was most significant in cells expressing the native form of the enzyme. We found that all cell lines accumulated lipid droplets within one day of starting palmitic acid exposures, but the cell lines expressing CYP2E1 in the mitochondria alone or in both organelles cleared the lipid droplets more quickly during serum starvation. Similarly, CYP2E1 expressed in HepG2 cells sensitized to a mild cytotoxicity from oleic acid. Interestingly, expression of CYP2E1 in the ER or in both organelles prevented an oleic acid-induced increase in mitochondrial respiration. Finally, we found that the palmitic acid cytotoxicity was not present in HepaRG hepatocyte-like cells even after differentiation and a more than 50-fold increase in CYP2E1 levels. Together, these findings may point to a cancer cell-specific role for CYP2E1 in lipotoxicity.

The finding that CYP2E1 expression sensitizes HepG2 cells to palmitic acid cytotoxicity supports previous work in independently derived CYP2E1-expressing HepG2 cell lines (named E47 and C34) (Nissar et al., 2015). That study also found that other hepatocellular carcinoma cell lines Hep3B and Huh7 show a similar dose-dependent cytotoxicity from palmitate, with high ~ 25 % cell death after 24 h exposure to 0.5 mM PA. In contrast to the cancer cells, we found the more "normal" HepaRG cells to be far less sensitive to PA-induced cytotoxicity. This was true in the undifferentiated state with low CYP2E1 levels and in the differentiated state with > 50-fold higher CYP2E1 levels. Along the same lines, another group found ~ 20 % cytotoxicity with 0.4 mM PA in primary hepatocytes compared to ~ 60 % cytotoxicity under the same conditions in HepG2 cells (Gomez-Torres et al., 2022), despite the fact that the primary hepatocytes express more CYP2E1 compared to HepG2 cells. The difference in the magnitude of cytotoxicity between that study and ours may be due to differences in dosing, as we complexed our free fatty acids with BSA prior to exposure. However, the overall trend is similar: cancer cells appear to be more sensitive to PA-induced cell death compared to a more normal hepatocyte cell. These findings may be relevant in the context of human cancer. Despite the role of CYP2E1 in producing ROS and promoting lipid peroxidation, high CYP2E1 levels in liver cancer are associated with a better prognosis (Fig. 7C). The differences may be the relative susceptibility to ferroptosis, as liver cancer is thought to be more sensitive to ferroptosis. Recent work in the liver cancer cell line LO-2 found that PA induces ferroptosis. Metabolites from the commensal gut microbe *Bifidobacterium bifidum* could block this ferroptosis, but not in the presence of CYP2E1 overexpression (Bu et al., 2024).

Previous studies have demonstrated that HepG2 cells take up exogenous palmitate and oleate from the media (Sung et al., 2004) and form lipid droplets (Eynaudi et al., 2021). CYP2E1 expression in the E47 HepG2 cells has been demonstrated to increase lipid droplet accumulation during long-term (4- to 8-day) ethanol exposure (Wu and Cederbaum, 2013; Wu et al., 2010). Supporting a role for CYP2E1 in fat accumulation, CYP2E1 genetic deletion in mice protects from alcohol (Lu et al., 2010)- and high fat diet (Zhang et al., 2022)-induced hepatic steatosis. In this study, we saw a similarly dramatic accumulation of lipids with fatty acid exposures at 24 h in all cell lines, regardless of CYP2E1 expression. However, with PA, we saw a return of lipid droplet levels to baseline after a longer 5-day exposure with serum starvation in cells expressing mitochondrial CYP2E1 (either the native sequence or the MT-specific cell lines). This may suggest a clearance of lipids that is promoted by mitochondrial CYP2E1. However, it remains to be determined in future studies the impact of direct fatty acid metabolism by CYP2E1 versus indirect effects on the lipid metabolism pathways (e.g. through PPAR signaling). Cells exposed to OA had a more similar decline in lipid droplets during the 5-day exposure period, regardless of CYP2E1 status. Together, these results suggest a potential lipid species-specific role for CYP2E1 in promoting lipid accumulation and clearance.

We also observed lipid species-specific functions of CYP2E1 for mitochondrial respiration. For palmitate, we found that PA exposure inhibited mitochondrial respiration for ~ 3 days in cells expressing the native CYP2E1 sequence. We also saw a significant ~ 60-hour inhibition of respiration in the ER-CYP2E1 line, although it was less dramatic than in the native form. A previous study found that in the HepG2 cell line, mitochondrial respiratory complex enzyme activity was inhibited after a 24 h palmitate exposure. This effect was ameliorated by inhibition of CYP2E1 with clomethiazole or by siRNA against CYP2E1(García-Ruiz et al., 2015). In that study, the authors observed a more dramatic effect of PA in the HepG2 parental line than we did, but they did not measure oxygen consumption rate. Unlike our results with PA, we saw an increase in oxygen consumption with oleic acid exposure only in the HepG2 cells lacking CYP2E1 and in cells expressing mitochondrial-targeted MT-CYP2E1. Cells expressing ER-CYP2E1 and the native CYP2E1 sequence showed no OA-induced increase in respiration. We assume the increase in OCR to be reflective of beta oxidation of the fatty

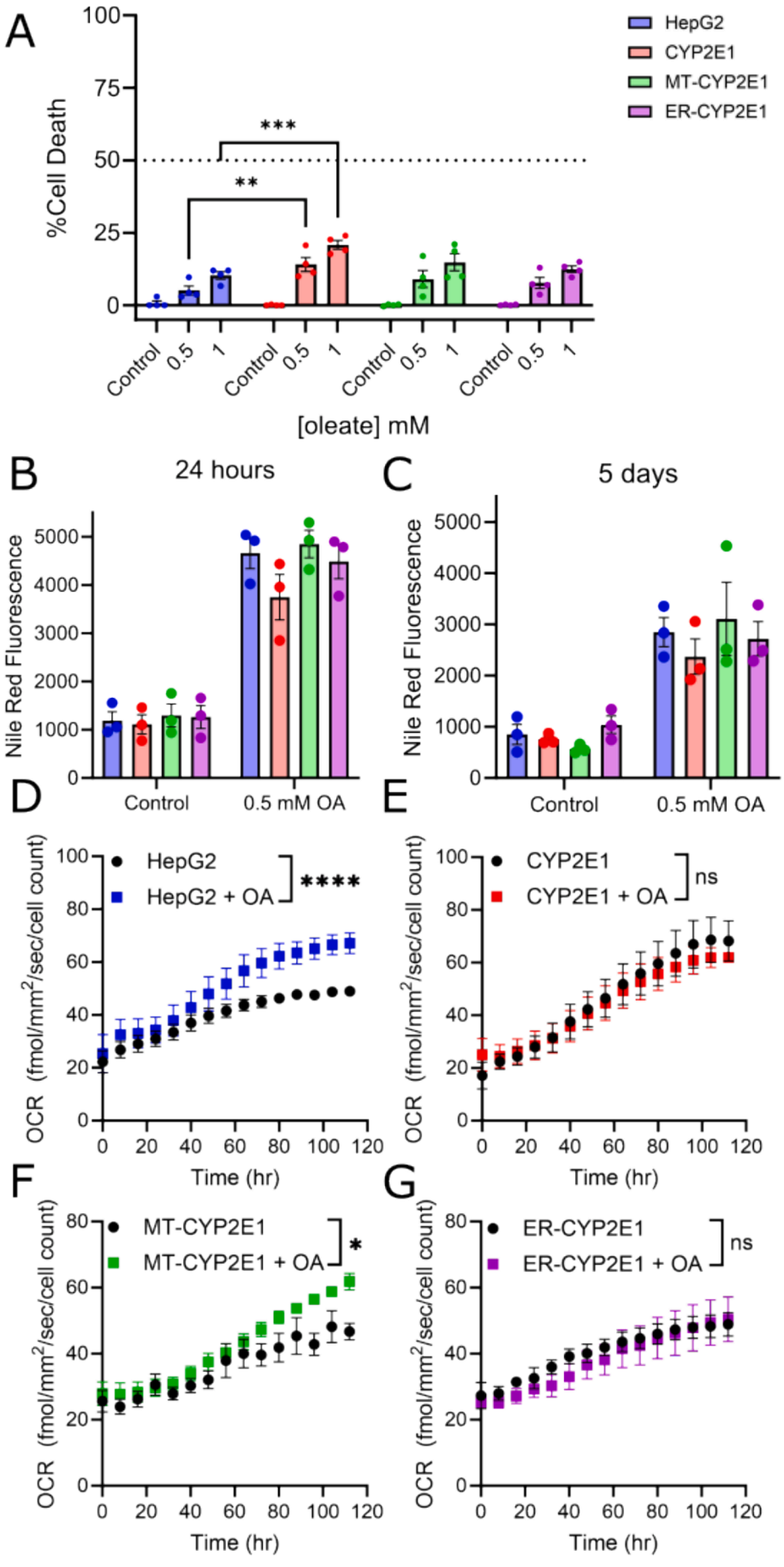

(caption on next page)

Fig. 3. Endoplasmic reticulum-localized CYP2E1 alters respiration following oleic acid exposure. Panel A, cell death following 24-hour exposure to oleic acid was determined by propidium iodide fluorescence (normalized to total fluorescence after addition of 1 % Triton X-100). **, $p < 0.01$, ***, $p < 0.001$, adjusted for multiple comparisons after 2-way ANOVA. Panels B-C, lipid droplets were measured following a 24 h (fed, panel B) or 5-day (serum starved, panel C) exposure to 0.5 mM OA. Briefly, following the exposure cells were fixed with 4 % paraformaldehyde and stained with Nile Red. **, $p < 0.01$, ***, $p < 0.001$, adjusted for multiple comparisons after 2-way ANOVA. Panels D-G, real-time oxygen consumption rate during exposure to 0.5 mM OA was measured using a Resipher device from Lucid Scientific. *, $p < 0.05$, ****, $p < 0.0001$ comparing area under the curve compiled from 3 independent replicates. (For interpretation of the references to colour in this figure legend, the reader is referred to the web version of this article.)

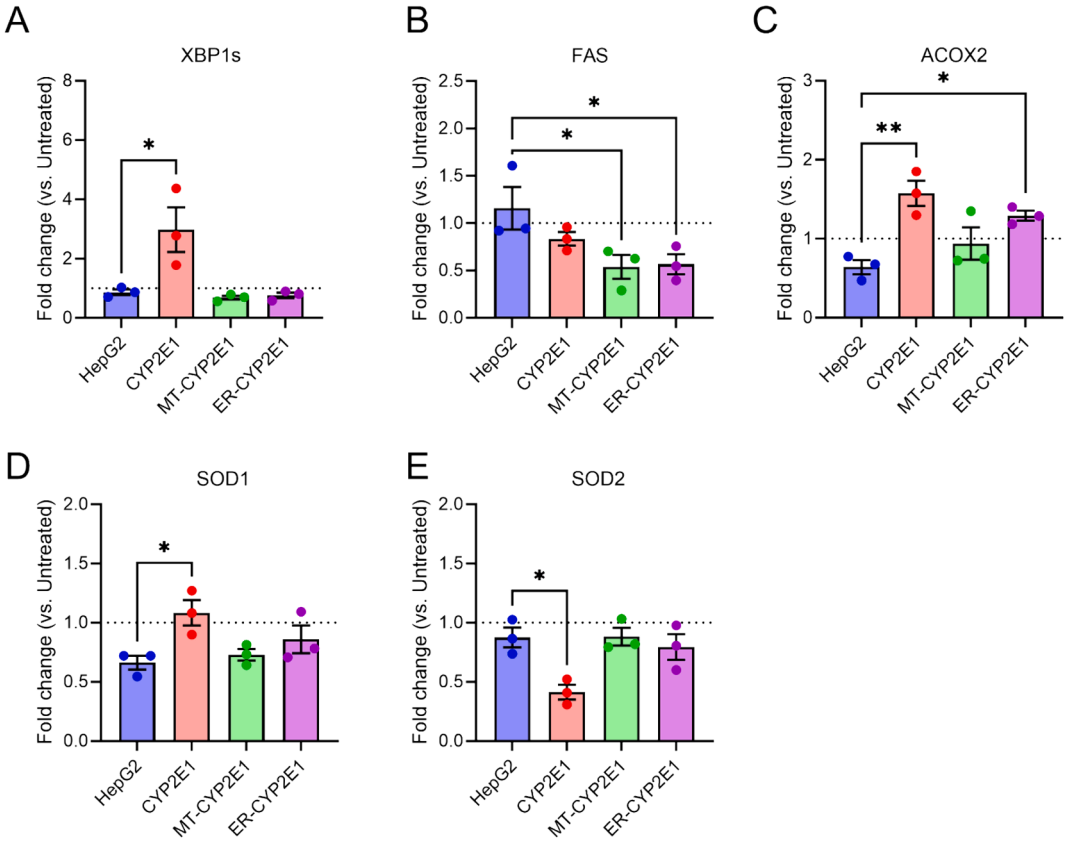

Fig. 4. Genes involved in ER stress, lipid handling, and oxidative stress are differentially expressed in CYP2E1-transduced HepG2 cells exposed to oleic acid. Cells were exposed to 0.5 mM oleic acid for 24 h, then cells were harvested and lysed and RNA was isolated. After cDNA synthesis, gene expression was determined by qPCR. The fold change was determined using the $2^{-\Delta\Delta Ct}$ method (normalized to β-actin and compared to the untreated cells) for each cell line and compared across cell lines. Panel A, spliced (activated) X-box binding protein 1, involved in ER stress response. Panel B, Fatty Acid Synthase, catalyzes the synthesis of fatty acids. Panel C, Acyl-CoA Oxidase 2, the rate-limiting enzyme in β-oxidation of branched, long-chain fatty acids. Panel D, Superoxide Dismutase 1, an enzyme localized throughout the cell that converts superoxide to hydrogen peroxide. Panel E, Superoxide Dismutase 2, an enzyme localized in the mitochondria that converts superoxide to hydrogen peroxide. Data shown are from 3 independent replicates. *, $p < 0.05$, **, −<0.01, adjusted for multiple comparisons after one-way ANOVA.

acids, but this remains to be explored further. CYP2E1 can directly metabolize oleic acid in the omega-1 position (Adas et al., 1998), albeit less efficiently than CYP4A enzymes. Therefore, it is possible that omega-1 hydroxylated fatty acids produced by the ER form of the enzyme (located on the ER facing the cytosol) have a different role compared to those produced in the mitochondria. To date, it is still unclear if the mitochondrial and ER forms of CYP2E1 have different fatty acid substrate metabolizing activities and the consequences of this on the cell.

Gene expression analysis following fatty acid exposures revealed few differentially expressed genes between HepG2 parental cells and the CYP2E1-expressing cells, but there was a consistent upregulation of ACOX2 in the CYP2E1 and ER-CYP2E1 HepG2 lines exposed to OA or the mixture of OA/PA. ACOX2 is the rate-limiting step for peroxisomal beta oxidation of branched long chain fatty acids and bile acid intermediates. This is an important enzyme for liver function and is downregulated in hepatocellular carcinoma (Zhang et al., 2021). Restoration of ACOX2 in hepatocellular carcinoma impedes tumor growth and upregulates the PPARα pathway, which is also linked to CYP2E1(Zhang et al., 2022). Together, these findings support a potential role for CYP2E1 in altering fatty acid pathways in cancer and should be explored further in future studies.

We acknowledge that our study had several important limitations. We used Nile Red for lipid quantification, which is widely used for *in vitro* quantification of neutral lipids (Greenspan et al., 1985) and has been extensively used for quantifying lipid droplets in HepG2 cells and other liver cells (McMillian et al., 2001; Weng et al., 2023; Huggett et al., 2022). However, Nile Red has a potential to have nonspecific interactions with other cellular lipids (Fowler et al., 1987). Several newer alternatives to Nile Red have emerged and may be more specific for neutral lipids (Suarez et al., 2020; Qiu and Simon, 2016). Therefore, these findings should be validated in future work with other probes. Another limitation is that we have not measured CYP2E1 protein content in each organelle in our study, although the ability of these N-terminal mutations to enrich CYP2E1 in each organelle was previously published (Bansal et al., 2013; Robin et al., 2002; Avadhani et al., 2011).

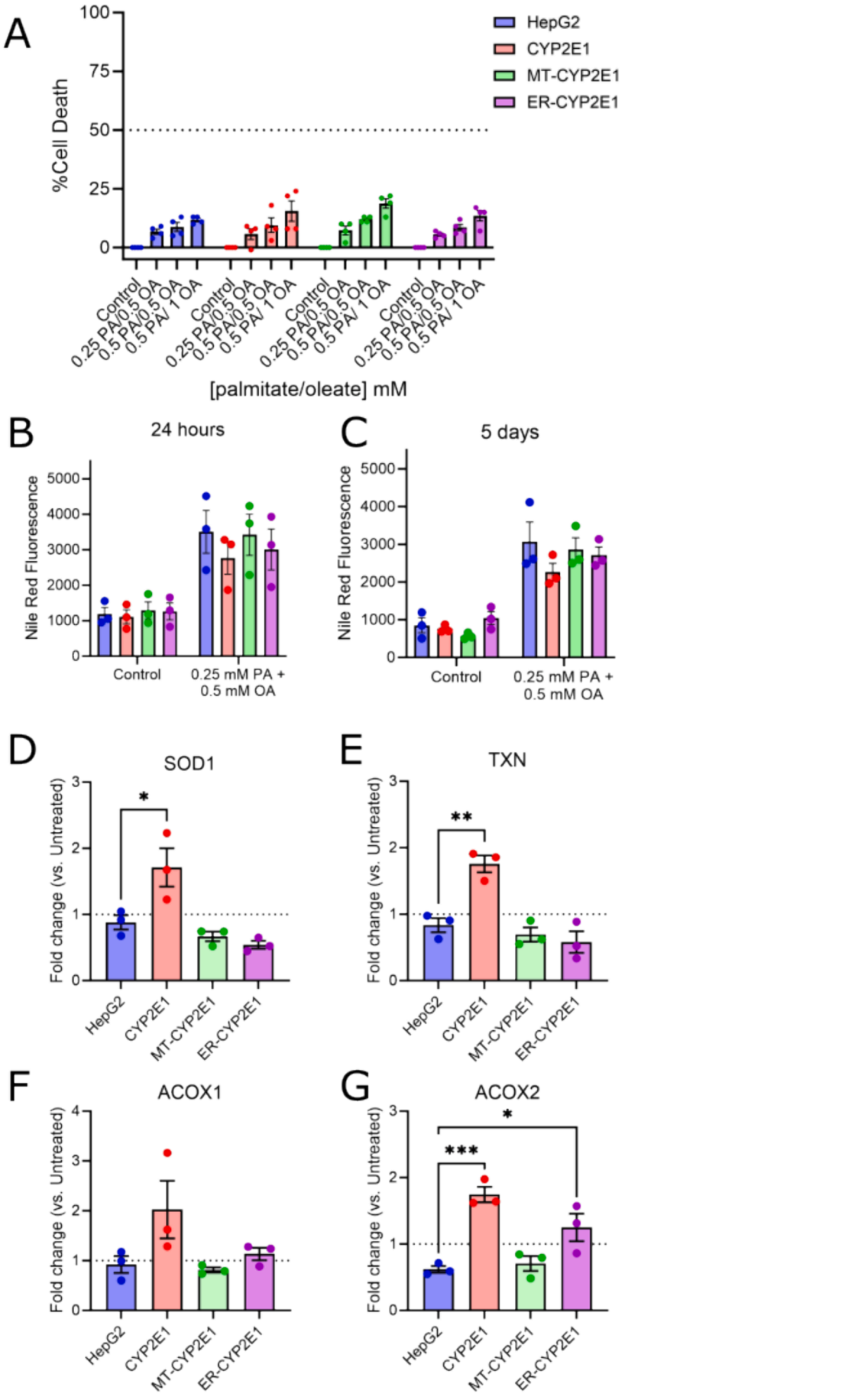

(caption on next page)

Fig. 5. HepG2 cells exposed to mixtures of palmitic and oleic acid are protected from cytotoxicity, and gene expression patterns are similar to oleic acid alone. Panel A, cell death following 24-hour exposure to mixtures of palmitic and oleic acid was determined by propidium iodide fluorescence (normalized to total fluorescence after addition of 1 % Triton X-100). Panels B-C, lipid droplets were measured following a 24 h (fed, panel B) or 5-day (serum starved, panel C) exposure to 0.25 mM PA and 0.5 mM OA. Briefly, following the exposure cells were fixed with 4 % paraformaldehyde and stained with Nile Red. For gene expression analysis, cells were exposed to 0.25 mM PA and 0.5 mM oleic acid for 24 h, then cells were harvested and lysed and RNA was isolated. After cDNA synthesis, gene expression was determined by qPCR. The fold change was determined using the $2^{-\Delta\Delta Ct}$ method (normalized to β-actin and compared to the untreated cells) for each cell line and compared across cell lines. Panel D, Superoxide Dismutase 1, an enzyme localized throughout the cell that converts superoxide to hydrogen peroxide. Panel E, Thioredoxin, catalyzes the reduction of oxidized cysteine residues and the cleavage of disulfide bonds. Panel F, Acyl-CoA Oxidase 1, the rate-limiting enzyme in peroxisomal strain-chain fatty acid β-oxidation. Panel G, Acyl-CoA Oxidase 2, the rate-limiting enzyme in β-oxidation of branched, long-chain fatty acids. Data shown are from 3 independent replicates. *, $p < 0.05$, **, −<0.01, adjusted for multiple comparisons after one-way ANOVA. (For interpretation of the references to colour in this figure legend, the reader is referred to the web version of this article.)

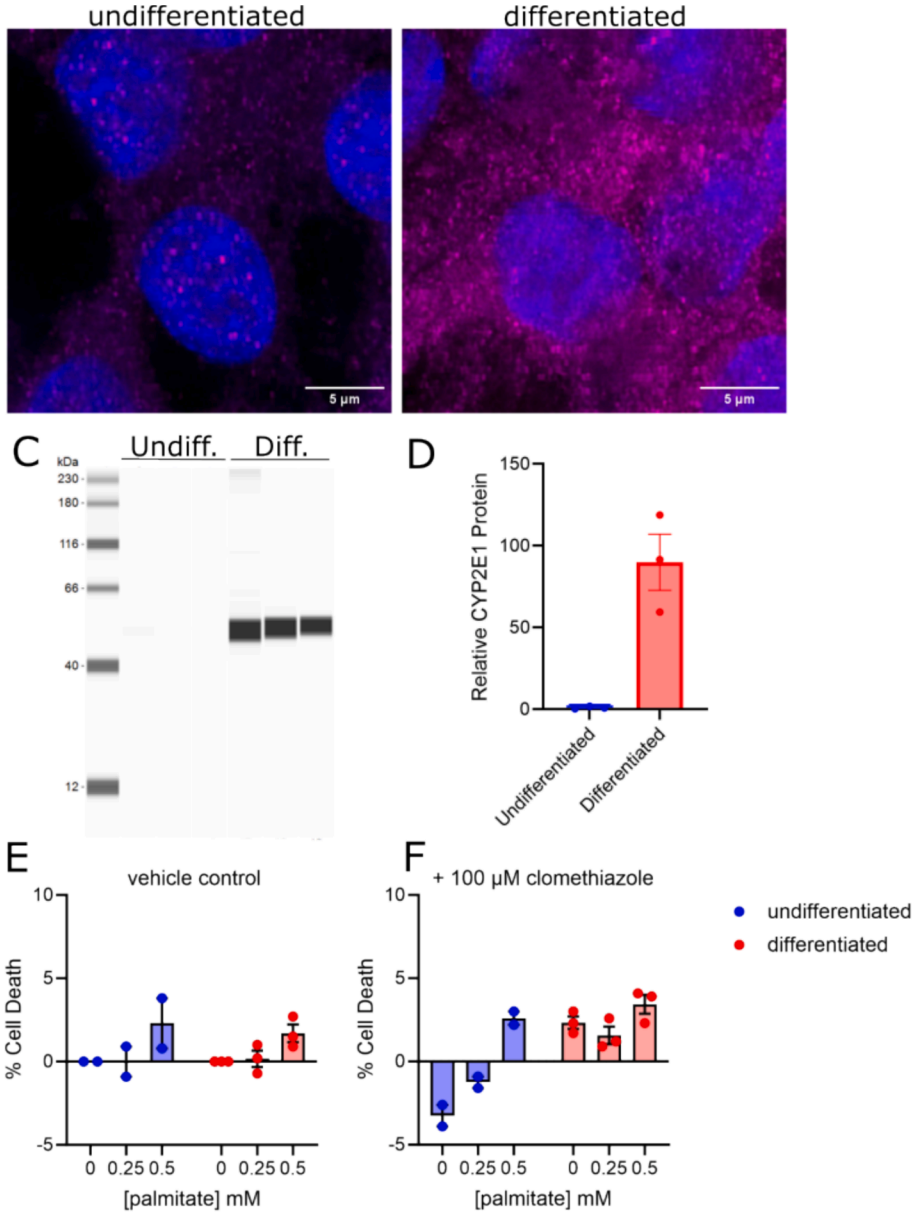

Fig. 6. HepaRG co-culture system accumulates abundant CYP2E1 protein during differentiation, but is not sensitive to palmitic acid cytotoxicity. Panels A-B, Immunofluorescent staining of CYP2E1 (magenta) and nuclei (DAPI, blue) in differentiated and undifferentiated HepaRG cells. HepaRG cells were cultured according to manufacturer protocols (Biopredic) and differentiated for 30 days on glass coverslips in 6-well plates. Undifferentiated cells were allowed to attach and recover from splitting for 3 days before fixation. Panels C-D, cells were differentiated and harvested for automated capillary-based Western Blot with the Jess system (Protein Simple). Panel C shows a rendering of bands for CYP2E1 at ~ 53 kDa only in the differentiated cells, while the quantitation (integration of peak areas) is shown in panel D, normalized to the undifferentiated cells. Panels E-F, cell death following 24-hour exposure to palmitic acid was determined by propidium iodide fluorescence (normalized to total fluorescence after addition of 1 % Triton X-100). (For interpretation of the references to colour in this figure legend, the reader is referred to the web version of this article.)

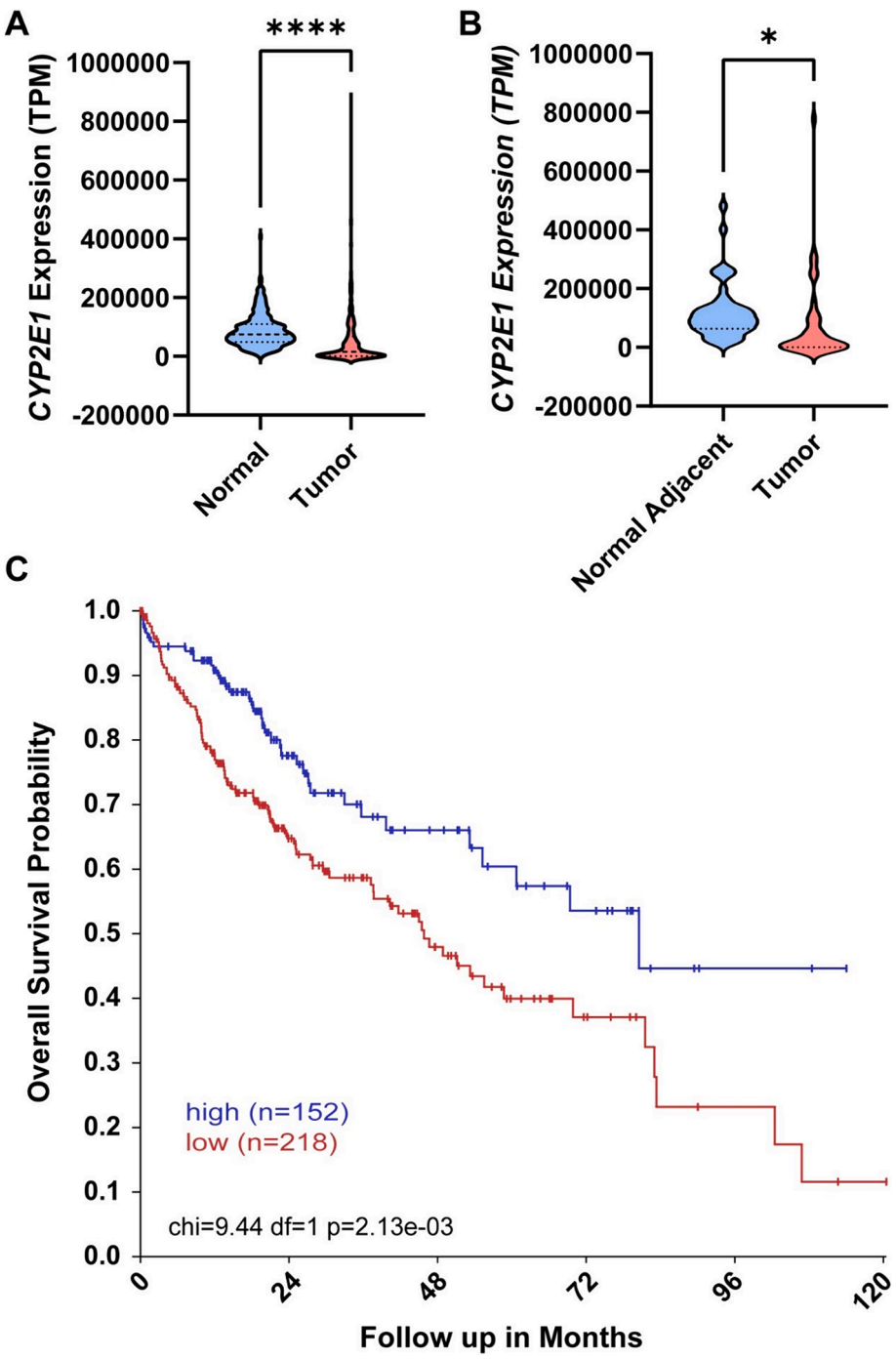

Fig. 7. CYP2E1 expression is decreased in liver hepatocellular carcinomas (LIHC) tumors and influences overall survival. Panel A, CYP2E1 mRNA expressed in transcript per million (TPM) in LIHC tumors and non-cancer control liver tissue. Panel B. CYP2E1 mRNA in LIHC tumors and paired tumor adjacent normal control liver tissue. Panel C. Survival curve of patients with high or low expressing LIHC tumors over 120 months. *$p < 0.05$, **$p < 0.001$, ***$p < 0.0001$, ***$p < 0.00001$, adjusted for multiple comparisons after one-way ANOVA.

Conclusion

Overall, this study showed that transgenic CYP2E1 expression in the well-differentiated hepatoma cell line HepG2 altered the response to palmitic and oleic acid. This was in sharp contrast to the insensitivity of HepaRG cells to palmitic acid. Overall, this work demonstrates the clear importance of CYP2E1 in dictating lipotoxicity and differential roles for the mitochondrial and ER forms of the enzyme.

Declaration of competing interest

The authors declare that they have no known competing financial interests or personal relationships that could have appeared to influence the work reported in this paper.

Data availability

Data will be made available on request.

Acknowledgements

This work was supported by the Advanced Imaging core of the Medical University of South Carolina Digestive Disease Research Core Center (P30 DK123704) and the Advanced Imaging core of the Medical University of South Carolina COBRE in Digestive and Liver Disease (P20 GM130457). The authors would like to acknowledge the kind assistance with imaging from Dr. Li Li and Dr. John Lemasters at MUSC. This work was supported by Pilot and Feasibility award from the Medical University of South Carolina Digestive Disease Research Core Center (P30 DK123704) and by the National Institute of General Medical Sciences R35-GM150843 (JHH, PI) and T32-GM132055 (EAA, trainee).

Appendix A. Supplementary data

Supplementary data to this article can be found online at https://doi.org/10.1016/j.crtox.2024.100195.

References

Adas, F., Berthou, F., Picart, D., Lozac'h, P., Beaugé, F., Amet, Y., 1998. Involvement of cytochrome P450 2E1 in the (omega-1)-hydroxylation of oleic acid in human and rat liver microsomes. J. Lipid Res. 39, 1210–1219.

Akakpo, J.Y., Ramachandran, A., Curry, S.C., Rumack, B.H., Jaeschke, H., 2022. Comparing N-acetylcysteine and 4-methylpyrazole as antidotes for acetaminophen overdose. Arch Toxicol 96, 453–465.

Avadhani, N.G., Sangar, M.C., Bansal, S., Bajpai, P., 2011. Bimodal targeting of cytochrome P450s to endoplasmic reticulum and mitochondria: the concept of chimeric signals. FEBS J. 278, 4218–4229.

Bansal, S., Liu, C.P., Sepuri, N.B., Anandatheerthavarada, H.K., Selvaraj, V., Hoek, J., Milne, G.L., Guengerich, F.P., Avadhani, N.G., 2010. Mitochondria-targeted cytochrome P450 2E1 induces oxidative damage and augments alcohol-mediated oxidative stress. J. Biol. Chem. 285, 24609–24619.

Bansal, S., Srinivasan, S., Anandasadagopan, S., Chowdhury, A.R., Selvaraj, V., Kalyanaraman, B., Joseph, J., Avadhani, N.G., 2012. Additive effects of mitochondrion-targeted cytochrome CYP2E1 and alcohol toxicity on cytochrome c oxidase function and stability of respirosome complexes. J Biol Chem 287, 15284–15297.

Bansal, S., Anandatheerthavarada, H.K., Prabu, G.K., Milne, G.L., Martin, M.V., Guengerich, F.P., Avadhani, N.G., 2013. Human cytochrome P450 2E1 mutations that alter mitochondrial targeting efficiency and susceptibility to ethanol-induced toxicity in cellular models. J. Biol. Chem. 288, 12627–12644.

Bartha, Á., Győrffy, B., 2021. TNMplot.com: A Web Tool for the Comparison of Gene Expression in Normal, Tumor and Metastatic Tissues. Int J Mol Sci 22.

Belfort, R., Harrison, S.A., Brown, K., Darland, C., Finch, J., Hardies, J., Balas, B., Gastaldelli, A., Tio, F., Pulcini, J., Berria, R., Ma, J.Z., Dwivedi, S., Havranek, R., Fincke, C., DeFronzo, R., Bannayan, G.A., Schenker, S., Cusi, K., 2006. A placebo-controlled trial of pioglitazone in subjects with nonalcoholic steatohepatitis. N. Engl. J. Med. 355, 2297–2307.

Bernauer, U., Vieth, B., Ellrich, R., Heinrich-Hirsch, B., Jänig, G.R., Gundert-Remy, U., 1999. CYP2E1-dependent benzene toxicity: the role of extrahepatic benzene metabolism. Arch Toxicol 73, 189–196.

Bondoc, F.Y., Bao, Z., Hu, W.Y., Gonzalez, F.J., Wang, Y., Yang, C.S., Hong, J.Y., 1999. Acetone catabolism by cytochrome P450 2E1: studies with CYP2E1-null mice. Biochem. Pharmacol. 58, 461–463.

Bu, G., Chen, G., Li, J., Wu, D., Liao, J., 2024. Bifidobacterium bifidum BGN4 fractions ameliorate palmitic acid-induced hepatocyte ferroptosis by inhibiting SREBP1-CYP2E1 pathway. J. Investig. Med. : Off. Publ. Am. Feder. Clin. Res. 72, 67–79.

Chen, F., Chandrashekar, D.S., Varambally, S., Creighton, C.J., 2019. Pan-cancer molecular subtypes revealed by mass-spectrometry-based proteomic characterization of more than 500 human cancers. Nat. Commun. 10, 5679.

Clarke, S.E., Baldwin, S.J., Bloomer, J.C., Ayrton, A.D., Sozio, R.S., Chenery, R.J., 1994. Lauric acid as a model substrate for the simultaneous determination of cytochrome P450 2E1 and 4A in hepatic microsomes. Chem Res Toxicol 7, 836–842.

Cui, W., Chen, S.L., Hu, K.Q., 2010. Quantification and mechanisms of oleic acid-induced steatosis in HepG2 cells. Am. J. Transl. Res. 2, 95–104.

Dicker, E., Cederbaum, A.I., 1991. Increased oxidation of dimethylnitrosamine in pericentral microsomes after pyrazole induction of cytochrome P-4502E1. Alcohol Clin Exp Res 15, 1072–1076.

Eynaudi, A., Díaz-Castro, F., Bórquez, J.C., Bravo-Sagua, R., Parra, V., Troncoso, R., 2021. Differential Effects of Oleic and Palmitic Acids on Lipid Droplet-Mitochondria Interaction in the Hepatic Cell Line HepG2. Front. Nutr. 8, 775382.

Fowler, S.D., Brown, W.J., Warfel, J., Greenspan, P., 1987. Use of nile red for the rapid in situ quantitation of lipids on thin-layer chromatograms. J. Lipid Res. 28, 1225–1232.

García-Ruiz, I., Solís-Muñoz, P., Fernández-Moreira, D., Muñoz-Yagüe, T., Solís-Herruzo, J.A., 2015. In vitro treatment of HepG2 cells with saturated fatty acids reproduces mitochondrial dysfunction found in nonalcoholic steatohepatitis. Dis. Model. Mech. 8, 183–191.

Gómez-Lechón, M.J., Donato, M.T., Martínez-Romero, A., Jiménez, N., Castell, J.V., O'Connor, J.E., 2007. A human hepatocellular in vitro model to investigate steatosis. Chem Biol Interact 165, 106–116.

Gomez-Torres, O., Amatya, S., Kamberov, L., Dhaibar, H.A., Khanna, P., Rom, O., Yurdagul Jr., A., Orr, A.W., Nunez, K., Thevenot, P., Cohen, A., Samant, H., Alexander, J.S., Burgos-Ramos, E., Chapa-Rodriguez, A., Cruz-Topete, D., 2022. SLAMF1 is expressed and secreted by hepatocytes and the liver in nonalcoholic fatty liver disease, *American journal of physiology*. Gastrointestinal and Liver Physiology 323, G177–G187.

Greenspan, P., Mayer, E.P., Fowler, S.D., 1985. Nile red: a selective fluorescent stain for intracellular lipid droplets. J Cell Biol 100, 965–973.

Harjumäki, R., Pridgeon, C. S., and Ingelman-Sundberg, M. (2021) CYP2E1 in Alcoholic and Non-Alcoholic Liver Injury. Roles of ROS, Reactive Intermediates and Lipid Overload, *International journal of molecular sciences 22*.

Hartman, J.H., Boysen, G., Miller, G.P., 2012. CYP2E1 metabolism of styrene involves allostery. Drug Metab. Dispos. 40, 1976–1983.

Hartman, J.H., Martin, H.C., Caro, A.A., Pearce, A.R., Miller, G.P., 2015. Subcellular localization of rat CYP2E1 impacts metabolic efficiency toward common substrates. Toxicology 338, 47–58.

Hartman, J.H., Miller, G.P., Meyer, J.N., 2017. Toxicological Implications of Mitochondrial Localization of CYP2E1. Toxicol. Res. 6, 273–289.

Hartman, J.H., Miller, G.P., Caro, A.A., Byrum, S.D., Orr, L.M., Mackintosh, S.G., Tackett, A.J., MacMillan-Crow, L.A., Hallberg, L.M., Ameredes, B.T., Boysen, G., 2017. 1,3-Butadiene-induced mitochondrial dysfunction is correlated with mitochondrial CYP2E1 activity in Collaborative Cross mice. Toxicology 378, 114–124.

Hong, J.Y., Pan, J.M., Gonzalez, F.J., Gelboin, H.V., Yang, C.S., 1987. The induction of a specific form of cytochrome P-450 (P-450j) by fasting. Biochem Biophys Res Commun 142, 1077–1083.

Huang, Y.S., Chern, H.D., Su, W.J., Wu, J.C., Chang, S.C., Chiang, C.H., Chang, F.Y., Lee, S.D., 2003. Cytochrome P450 2E1 genotype and the susceptibility to antituberculosis drug-induced hepatitis, *Hepatology (Baltimore*, Md.) 37, 924–930.

Huggett, Z.J., Smith, A., De Vivo, N., Gomez, D., Jethwa, P., Brameld, J.M., Bennett, A., Salter, A.M., 2022. A Comparison of Primary Human Hepatocytes and Hepatoma Cell Lines to Model the Effects of Fatty Acids. Fructose and Glucose on Liver Cell Lipid Accumulation, Nutrients, p. 15.

Khemawoot, P., Yokogawa, K., Shimada, T., Miyamoto, K., 2007. Obesity-induced increase of CYP2E1 activity and its effect on disposition kinetics of chlorzoxazone in Zucker rats. Biochem. Pharmacol. 73, 155–162.

Lieber, C.S., DeCarli, L.M., 1970. Hepatic microsomal ethanol-oxidizing system. In Vitro Characteristics and Adaptive Properties in Vivo. J. Biol. Chem. 245, 2505–2512.

Lu, Y., Wu, D., Wang, X., Ward, S.C., Cederbaum, A.I., 2010. Chronic alcohol-induced liver injury and oxidant stress are decreased in cytochrome P4502E1 knockout mice and restored in humanized cytochrome P4502E1 knock-in mice. Free Radic. Biol. Med. 49, 1406–1416.

Lück, C., Haitjema, C., Heger, C., 2021. Simple Western: Bringing the Western Blot into the Twenty-First Century. Methods Mol Biol 2261, 481–488.

Marion, M.J., Hantz, O., Durantel, D., 2010. The HepaRG cell line: biological properties and relevance as a tool for cell biology, drug metabolism, and virology studies. Methods Mol Biol 640, 261–272.

McMillian, M.K., Grant, E.R., Zhong, Z., Parker, J.B., Li, L., Zivin, R.A., Burczynski, M.E., Johnson, M.D., 2001. Nile Red binding to HepG2 cells: an improved assay for in vitro studies of hepatosteatosis. In Vitr. Mol. Toxicol. 14, 177–190.

Michaut, A., Le Guillou, D., Moreau, C., Bucher, S., McGill, M.R., Martinais, S., Gicquel, T., Morel, I., Robin, M.A., Jaeschke, H., Fromenty, B., 2016. A cellular model to study drug-induced liver injury in nonalcoholic fatty liver disease: Application to acetaminophen. Toxicol. Appl. Pharmacol. 292, 40–55.

Miller, G.P., 2008. Advances in the interpretation and prediction of CYP2E1 metabolism from a biochemical perspective. Expert Opin. Drug Metab. Toxicol. 4, 1053–1064.

Neve, E.P., Ingelman-Sundberg, M., 1999. A soluble NH(2)-terminally truncated catalytically active form of rat cytochrome P450 2E1 targeted to liver mitochondria (1). FEBS Lett. 460, 309–314.

Nieusma, J.L., Claffey, D.J., Koop, D.R., Chen, W., Peter, R.M., Nelson, S.D., Ruth, J.A., Ross, D., 1998. Oxidation of 1,3-butadiene to (R)- and (S)-butadiene monoxide by purified recombinant cytochrome P450 2E1 from rabbit, rat and human. Toxicol Lett 95, 123–129.

Nissar, A.U., Sharma, L., Tasduq, S.A., 2015. Palmitic acid induced lipotoxicity is associated with altered lipid metabolism, enhanced CYP450 2E1 and intracellular calcium mediated ER stress in human hepatoma cells. Toxicol. Res. 4, 1344–1358.

Qiu, B., and Simon, M. C. (2016) BODIPY 493/503 Staining of Neutral Lipid Droplets for Microscopy and Quantification by Flow Cytometry, *Bio Protoc 6*.

Raucy, J.L., Lasker, J.M., Kraner, J.C., Salazar, D.E., Lieber, C.S., Corcoran, G.B., 1991. Induction of cytochrome P450IIE1 in the obese overfed rat. Mol. Pharmacol. 39, 275–280.

Roberts, B.J., Shoaf, S.E., Jeong, K.S., Song, B.J., 1994. Induction of CYP2E1 in Liver, Kidney, Brain and Intestine During Chronic Ethanol Administration and Withdrawal: Evidence That CYP2E1 Possesses a Rapid Phase Half-Life of 6 Hours or Less. Biochem. Biophys. Res. Commun. 205, 1064–1071.

Robin, M.A., Anandatheerthavarada, H.K., Fang, J.K., Cudic, M., Otvos, L., Avadhani, N. G., 2001. Mitochondrial targeted cytochrome P450 2E1 (P450 MT5) contains an intact N terminus and requires mitochondrial specific electron transfer proteins for activity. J. Biol. Chem. 276, 24680–24689.

Robin, M.A., Anandatheerthavarada, H.K., Biswas, G., Sepuri, N.B., Gordon, D.M., Pain, D., Avadhani, N.G., 2002. Bimodal targeting of microsomal CYP2E1 to mitochondria through activation of an N-terminal chimeric signal by cAMP-mediated phosphorylation. J. Biol. Chem. 277, 40583–40593.

Sanyal, A.J., Campbell-Sargent, C., Mirshahi, F., Rizzo, W.B., Contos, M.J., Sterling, R.K., Luketic, V.A., Shiffman, M.L., Clore, J.N., 2001. Nonalcoholic steatohepatitis: association of insulin resistance and mitochondrial abnormalities. Gastroenterology 120, 1183–1192.

Sharma, S., Mells, J.E., Fu, P.P., Saxena, N.K., Anania, F.A., 2011. GLP-1 analogs reduce hepatocyte steatosis and improve survival by enhancing the unfolded protein response and promoting macroautophagy. PLoS One 6, e25269.

Suarez, S.I., Warner, C.C., Brown-Harding, H., Thooft, A.M., VanVeller, B., Lukesh, J.C., 2020. Highly selective staining and quantification of intracellular lipid droplets with a compact push-pull fluorophore based on benzothiadiazole. Org. Biomol. Chem. 18, 495–499.

Sung, M., Kim, I., Park, M., Whang, Y., Lee, M., 2004. Differential effects of dietary fatty acids on the regulation of CYP2E1 and protein kinase C in human hepatoma HepG2 cells. J. Med. Food 7, 197–203.

van Rongen, A., Valitalo, P.A., Peeters, M.Y., Boerma, D., Huisman, F.W., van Ramshorst, B., van Dongen, E.P., van den Anker, J.N., Knibbe, C.A., 2016. Morbidly Obese Patients Exhibit Increased CYP2E1-Mediated Oxidation of Acetaminophen. Clin. Pharmacokinet. 55, 833–847.

Wan, J., Ernstgard, L., Song, B.J., Shoaf, S.E., 2006. Chlorzoxazone metabolism is increased in fasted Sprague-Dawley rats. J. Pharm. Pharmacol. 58, 51–61.

Wang, S., Xing, G., Li, F., Yang, B., Zhang, Y., Aschner, M., and Lu, R. (2022) Fasting Enhances the Acute Toxicity of Acrylonitrile in Mice via Induction of CYP2E1, *Toxics 10*.

Wang, Z., Hall, S.D., Maya, J.F., Li, L., Asghar, A., Gorski, J.C., 2003. Diabetes mellitus increases the in vivo activity of cytochrome P450 2E1 in humans. Br. J. Clin. Pharmacol. 55, 77–85.

Wanninger, J., Neumeier, M., Hellerbrand, C., Schacherer, D., Bauer, S., Weiss, T.S., Huber, H., Schäffler, A., Aslanidis, C., Schölmerich, J., Buechler, C., 2011. Lipid accumulation impairs adiponectin-mediated induction of activin A by increasing TGFbeta in primary human hepatocytes. Biochim Biophys Acta 1811, 626–633.

Weltman, M.D., Farrell, G.C., Hall, P., Ingelman-Sundberg, M., Liddle, C., 1998. Hepatic cytochrome P450 2E1 is increased in patients with nonalcoholic steatohepatitis, *Hepatology (Baltimore.* Md.) 27, 128–133.

Weng, S.W., Wu, J.C., Shen, F.C., Chang, Y.H., Su, Y.J., Lian, W.S., Tai, M.H., Su, C.H., Chuang, J.H., Lin, T.K., Liou, C.W., Chu, T.H., Kao, Y.H., Wang, F.S., Wang, P.W., 2023. Chaperonin counteracts diet-induced non-alcoholic fatty liver disease by aiding sirtuin 3 in the control of fatty acid oxidation. Diabetologia 66, 913–930.

Wu, D., Cederbaum, A.I., 2013. Inhibition of autophagy promotes CYP2E1-dependent toxicity in HepG2 cells via elevated oxidative stress, mitochondria dysfunction and activation of p38 and JNK MAPK. Redox Biol. 1, 552–565.

Wu, D., Wang, X., Zhou, R., Cederbaum, A., 2010. CYP2E1 enhances ethanol-induced lipid accumulation but impairs autophagy in HepG2 E47 cells. Biochem Biophys Res Commun 402, 116–122.

Yadav, S., Dhawan, A., Singh, R.L., Seth, P.K., Parmar, D., 2006. Expression of constitutive and inducible cytochrome P450 2E1 in rat brain. Mol. Cell. Biochem. 286, 171–180.

Zhang, Y., Yan, T., Wang, T., Liu, X., Hamada, K., Sun, D., Sun, Y., Yang, Y., Wang, J., Takahashi, S., Wang, Q., Krausz, K.W., Jiang, C., Xie, C., Yang, X., Gonzalez, F.J., 2022. Crosstalk between CYP2E1 and PPARα substrates and agonists modulate adipose browning and obesity. Acta Pharmaceut. Sinica B 12, 2224–2238.

Zhang, Q., Zhang, Y., Sun, S., Wang, K., Qian, J., Cui, Z., Tao, T., Zhou, J., 2021. ACOX2 is a prognostic marker and impedes the progression of hepatocellular carcinoma via PPARα pathway. Cell Death Dis. 12, 15.